Heliyon 7 (2021) e07456

Contents lists available at ScienceDirect

Heliyon

journal homepage: www.cell.com/heliyon

Research article

Doxorubicin induces dysregulation of AMPA receptor and impairs hippocampal synaptic plasticity leading to learning and memory deficits

Ahmad H. Alhowail [a,1], Priyanka D. Pinky [b,1], Matthew Eggert [b], Jenna Bloemer [b,e], Lauren N. Woodie [c,d], Manal A. Buabeid [f], Subhrajit Bhattacharya [b,g], Shanese L. Jasper [b], Dwipayan Bhattacharya [h], Muralikrishnan Dhanasekaran [b,g], Martha Escobar [i], Robert D. Arnold [b,g,**], Vishnu Suppiramaniam [b,g,*]

[a] Department of Pharmacology and Toxicology, Qassim University, Buraydah, Saudi Arabia
[b] Department of Drug Discovery and Development, Auburn University, Auburn, Alabama, USA
[c] Department of Nutrition, Dietetics and Hospitality Management, College of Human Sciences, Auburn University, Auburn, Alabama, USA
[d] Institute for Diabetes, Obesity and Metabolism, Division of Endocrinology, Diabetes and Metabolism, Department of Medicine, University of Pennsylvania Perelman School of Medicine, Philadelphia, PA, USA
[e] Department of Pharmaceutical and Biomedical Sciences, Touro College of Pharmacy, New York, NY, USA
[f] College of Pharmacy and Health Sciences, Ajman University, Ajman, United Arab Emirates
[g] Center for Neuroscience Initiative, Auburn University, Auburn, AL, USA
[h] Department of Pharmacology, Lake Erie College of Osteopathic Medicine, PA, USA
[i] Department of Psychology, Oakland University, Rochester, MI, USA

HIGHLIGHTS

- Doxorubicin is associated with "chemobrain," a long-term cancer related cognitive impairment.
- Doxorubicin treatment results in hippocampus-dependent learning and memory deficits.
- Impairment in hippocampal long-term potentiation is accompanied with reduced functionality of glutamate subtype AMPA receptor.
- Dysregulation of CaMKII, BDNF, ERK, and AKT protein signaling leading to learning and memory impairment.

ARTICLE INFO

Keywords:
Doxorubicin
Chemobrain
Long-term potentiation
AMPA
Cognitive deficits
Synaptic plasticity

ABSTRACT

Doxorubicin (Dox) is a chemotherapeutic agent used widely to treat a variety of malignant cancers. However, Dox chemotherapy is associated with several adverse effects, including "chemobrain," the observation that cancer patients exhibit through learning and memory difficulties extending even beyond treatment. This study investigated the effect of Dox treatment on learning and memory as well as hippocampal synaptic plasticity. Dox-treated mice (5 mg/kg weekly x 5) demonstrated impaired performance in the Y-maze spatial memory task and a significant reduction in hippocampal long-term potentiation. The deficit in synaptic plasticity was mirrored by deficits in the functionality of synaptic `α-amino-3- hydroxy-5-methyl-4-isoxazolepropionic acid receptor (AMPAR) channels, including reduced probability of opening, decreased dwell open time, and increased closed times. Furthermore, a reduction in the AMPAR subunit GluA1 level, its downstream signaling molecule Ca^2+/calmodulin-dependent protein kinase (CaMKII), and brain-derived neurotrophic factor (BDNF) were observed. This was also accompanied by an increase in extracellular signal regulated kinase (ERK) and protein kinase B (AKT) activation. Together these data suggest that Dox-induced cognitive impairments are at least partially due to alterations in the expression and functionality of the glutamatergic AMPAR system.

* Corresponding author.
** Corresponding author.
E-mail addresses: rda0007@auburn.edu (R.D. Arnold), suppivd@auburn.edu (V. Suppiramaniam).
[1] Equal contribution.

https://doi.org/10.1016/j.heliyon.2021.e07456
Received 15 February 2021; Received in revised form 10 June 2021; Accepted 28 June 2021

1. Introduction

In the past decade, significant advances have been made in the early detection and successful treatment of cancer. Chemotherapy, while an effective treatment for most cancers, has many adverse effects. Cognitive deficits have been reported in up to 75% of patients receiving chemotherapy for breast cancer (Jenkins et al., 2006). These cognitive effects, which include but are not limited to impairment in thinking, concentration, learning new skills, remembering and/or memorizing, have become so ubiquitous in chemotherapy treatment that they have earned the name "chemobrain" (Lambert et al., 2018; Lange and Joly, 2017; "Understanding Post-Treatment 'Chemobrain' - National Cancer Institute," 2017). Doxorubicin (Dox) is an anthracycline compound widely used to treat a number of cancers, including breast cancers, prostate cancers, and osteosarcomas (Thorn et al., 2011). Dox acts in part by inhibiting topoisomerase II, which is essential for DNA synthesis (Bodley et al., 1989; Zhang et al., 2012). Although Dox is effective against cancer growth, its use is limited by several well-known adverse effects, including cardiotoxicity, nephrotoxicity, and hepatotoxicity (Briones and Woods, 2011a; Damodar et al., 2014; Ichikawa et al., 2014; S. Lahoti et al., 2012). Recently, Dox has also been linked to "chemobrain" (Aluise et al., 2010; Kesler and Blayney, 2016). Although much of the research associated with chemobrain has been anecdotal and not focused on the underlying pathophysiology, a few studies have attempted to investigate the molecular mechanisms associated with chemotherapy induced memory dysfunction (Antkiewicz-Michaluk et al., 2016; Briones and Woods, 2011b; Salas-Ramirez et al., 2015; Wu et al., 2016). Dox cannot readily penetrate the intact blood-brain barrier (BBB) because it is ionized under physiological conditions in the blood and a substrate for the BBB efflux transporter, P-glycoprotein (Pgp) (Arnold et al., 2005; Christie et al., 2012; Keeney et al., 2018; Thomas et al., 2017). However, Dox treatment can increases the production of reactive oxygen species (ROS), leading to increased lipid peroxidation (Alhowail et al., 2019), thus facilitating the disruption of the BBB and impaired synaptic plasticity. Additionally, subnanomolar amounts of some chemotherapeutic agents that don't readily cross the BBB, including Dox have been found in the central nervous system (CNS) (Arnold et al., 2004) and can cause neuronal apoptosis, reduced neuronal division in the brain (Ahles and Saykin, 2007) and impaired synaptic plasticity (Alhowail et al., 2019). Although Dox-induced alterations in hippocampal memory have been observed (Alhowail et al., 2019; Keeney et al., 2018; Salas-Ramirez et al., 2015), the mechanism by which Dox impairs excitatory neurotransmission and plasticity in the hippocampus, eventually leading memory deficits, remains to be established.

Glutamate activity in the hippocampus is essential for the formation of new memories, and the two major glutamate receptors associated with memory are α-amino-3-hydroxy-5-methyl-4-isoxazole propionic acid receptors (AMPAR) and N-methyl-D-aspartate receptors (NMDAR) (Riedel et al., 2003). Each receptor is made up of several subunits, (GluA1-4 for AMPARs, and primarily GluN1, 2A-D, and more recently discovered GluN3 subunits for NMDARs) and these receptors act as the primary transducers of excitatory neurotransmission in the hippocampus and are implicated in many neurodegenerative disorders (Bhattacharya et al., 2018; Ogden et al., 2017; Traynelis et al., 2010). Postsynaptic response can be increased either by increasing the number of postsynaptic receptors or by increasing their single channel conductance ("Glutamate receptors | Centre for Synaptic Plasticity | University of Bristol," 2020; Huganir and Nicoll, 2013; Lüscher and Malenka, 2012). Ca^{2+} influx through NMDARs plays an important role in memory processes by activating the Ca^{2}+/calmodulin-dependent protein kinase (CaMKII) pathway (Fink and Meyer, 2002), which in turn leads to increased expression of AMPARs/NMDARs. AMPAR trafficking and stabilization on the postsynaptic surface is crucial for maintenance of synaptic plasticity which is dependent on various auxiliary proteins (Bissen et al., 2019a; Henley, 2003). Stargazin is a transmembrane protein which interacts with PSD-95 or related PDZ proteins for synaptic targeting of AMPARs and delivery to the surface membrane (Chen et al., 2000). This role of stargazin is important since stargazin lacking the PDZ-binding domain disrupts AMPARs mediated synaptic responses (Chen et al., 2000). Thus altered expression and/or activity of AMPAR, NMDAR, or both can result in changes in synaptic plasticity (Huganir and Nicoll, 2013; Lüscher and Malenka, 2012; Malinow, 2003). Therefore, the glutamatergic system presents a potential target for the treatment of chemotherapy-induced cognitive dysfunction.

Here, we investigated the impact of Dox treatment on synaptic plasticity and memory in athymic NCr (T-cell deficient, partially immunocompromised) nude mice, a standard murine model for cancer studies. Specifically, we sought to examine the correlation between AMPAR expression/function and memory in Dox-treated mice. Memory function was assessed in control mice and Dox-treated using the delayed version of the Y maze, which can be used to assess working and reference spatial memory in rodents (Kraeuter et al., 2019) and is sensitive to deficits in hippocampal function (Conrad et al., 1996; Sarnyai et al., 2000). Hippocampal long-term potentiation (LTP), which can be characterized as the cellular correlate of learning and memory (Lüscher and Malenka, 2012), was used to evaluate hippocampal synaptic plasticity. Furthermore, hippocampal glutamatergic AMPAR expression and function were assessed to determine potential mechanisms underlying Dox-induced alterations in LTP. Additionally, we investigated the downstream signaling pathways by which glutamate-mediated synaptic deficits might occur. Understanding the underlying mechanistic effects of Dox on glutamatergic hippocampal function may help to identify novel therapeutics for the prevention or management of chemotherapy-induced neurotoxicity. Thus, this study helps to fill an important gap in the existing literature by elucidating the signaling mechanisms of cognitive deficits caused by Dox and assessing protein targets that may prove essential in the treatment strategies against "chemobrain."

2. Materials and methods

2.1. Animal subjects

6-week-old athymic (T-cell deficient, partially immunocompromised) male mice (NCr nude; Taconic Biosciences, Inc.) were housed in pathogen-free conditions a 12h light: 12h dark cycle, temperature controlled (22–24 °C) room and provided with ad libitum access to food and water. Animal care and husbandry procedures were approved by the Institutional Animal Care and Use Committee (IACUC) and conformed to the NIH Guide for the Care and Use of Laboratory Animals (8^{th} Ed.). For the Dox-treated group, mice were treated with Dox 5 mg/kg via an intravenous (I.V) tail vein injection weekly for a total of 5 doses. Dox was obtained from Cell Signaling Technology (Danvers, MA) and solution was prepared fresh mixed with saline and filtered before injection. An equivalent amount of vehicle (0.9% w/v saline) was administrated to the remaining animals, which were used as control animals. 5–6 mice per group (Dox and Control) were used for the behavioral task. A separate set of animals (behaviorally naive) were used for electrophysiological ($n = 4$ mice per group), synaptosome preparation ($n = 6$ mice per group) and immunoblot studies ($n = 3$–4 mice per group), since stress due to behavioral manipulations may interfere with LTP (Korz and Frey, 2003) and alter AMPA receptor subunits expression and signaling (Aguayo et al., 2018). Figure 1 provides an illustration on experimental timeline.

2.2. Chemicals and reagents

For artificial cerebrospinal fluid (aCSF) preparation, NaCl (S7653) KCl (P9333), $CaCl_2$(C5080), NaH_2PO4(S8282), $NaHCO_3$(S5761), sucrose (S7903), and ascorbate (A5960) were purchased from Sigma- Aldrich (St. Louis, MO). The concentration of the ingredients in the freshly prepared aCSF were: (in mM) 124 NaCl, 3 KCl, 1.5 MgSO47H20, 1.2 NaH2PO4, 2.4 CaCl2, 25 NaHCO3, and 10 D-Glucose. Neuronal Protein Extraction Reagent (N-PER) (Cat# 87792) was purchased from Thermo Fisher

Scientific Inc. (Rockford, IL). 4X Laemmli buffer and Tris-buffered saline were purchased from Bio-Rad (Hercules, CA). Antibodies were purchased from Cell Signaling Technology (Danvers, MA). Ultrapure water was obtained from a Millipore Milli-Q synthesis system. (Billerica, MA). $MgSO_4$ (AC M65500) and glucose (97061-164) were purchased from Acros organics and VWR, respectively.

2.3. Y-maze test

The Y-maze (Figure 1A) was used as a task for assessing working memory and spatial memory function in Dox and vehicle treated (control) mice as described previously (Bannerman et al., 2014). The Y-maze is a spatial memory test that capitalizes on rodents' tendency to explore new environments. Because animals are not required to acquire a new behavior, no appetitive or aversive stimuli are required to assess behavior. The apparatus for Y-maze consists of 3 arms made of opaque plastic and positioned at 120° to each other. Each arm was measured 7.5 cm × 38 cm x 15 cm (w x l x h). The arms were equally illuminated with dim overhead lights, and each arm was fitted with a distinct cue immediately above the arm's back wall. Testing sessions were recorded with a video camera placed above the center of the maze, and the recordings were used for later analysis by a scorer blind to the treatment subjects received. Mice were 12 weeks of age at the initiation of training sessions. The three arms of the maze were designated as the Entry, Novel, and Known arms, and a distinct extra-maze cue was placed at the end corner of each arm, approximately 5 cm above the wall. Arm designation was counterbalanced within groups. During the 15-minutes long training session, mice could explore only 2 arms: the arm where they were placed (Entry arm) and one (Known arm) of the two other arms. The third arm (Novel arm) was occluded by an opaque divider. After the task, mice were returned to their home cages. After 3 h had elapsed, the mice were placed back in the maze for a test session, during which all arms open. Mice were placed back in the Entry arm, and allowed to explore the maze for 10 min. The maze was thoroughly cleaned using a 20% (v/v) alcohol solution between subjects. Using a delayed testing strategy allowed for assessment of animals' working spatial memory (spontaneous alternations) and reference spatial memory (number of entries and time spent in each arm) (Kraeuter et al., 2019). An arm entry was scored when the entire mouse's body had entered an arm; time spent in the arm was scored from the moment the entire mouse's body had entered the arm until the entire mouse's body had exited the arm. Scores for the Known and Entry arms were averaged to obtain a score for the Familiar arm, which was contrasted to the scores for the Novel arm. Percent entries and percent dwell time were calculated as a proportion of total number of entries or total dwell in arms, respectively; this means that chance percent entries or percent dwell time was 33% for the Novel and Familiar arms. Spontaneous alternations (any sequence of consecutive entries into three different arms) were scored to assess working memory, were calculated as the number of alternations divided by the total possible alternations (total number of arm entries minus 2) and multiplied by 100.

2.4. Preparation of acute hippocampal slices

4 weeks after treatment with Dox, mice were euthanized with CO_2. As soon as mice stopped spontaneous breathing (within 3–4 min of CO_2 inhalation), brains were surgically excised following decapitation. The brain was then washed with ice cold oxygenated cutting solution (NaCl 85mM, KCl 2.5mM, $MgSO_4$ 4.0mM, $CaCl_2$ 0.5mM, NaH_2PO_4 1.25mM, $NaHCO_3$ 25mM, glucose 25mM, sucrose 75mM, and ascorbate 0.5mM) and transverse slices were prepared (350 μm thick). The slices were preserved in a holding chamber, submerged in oxygenated aCSF (in mM, 124 NaCl, 3 KCl, 1.5 $MgSO_4$7H20, 1.2 NaH2PO4, 2.4 $CaCl_2$, 25 NaHCO3, and 10 D-Glucose bubbled with 95% O_2/5% CO_2) (Bloemer et al., 2019; Petrisko et al., 2020).

2.5. Extracellular field recordings

Hippocampal slices were transferred into a recording chamber, under a microscope (Nikon SMZ 745T microscope). This recording chamber was submerged with oxygenated aCSF maintained at 34 °C in a continuous perfusion manner. A bipolar stimulating electrode was placed on CA3 region and a recording glass microelectrode (World Precision Instruments, Sarasota, Florida), filled with aCSF solution was placed on the stratum radiatum of CA1 region of hippocampus to record field excitatory postsynaptic potentials (fEPSP) from the Schaffer collateral pathway. Input-output responses were represented by fEPSP slopes and fiber volley (FV) amplitudes at increasing stimulus intensities. For LTP recording, stimulus intensity was set at 50% of the maximum amplitude

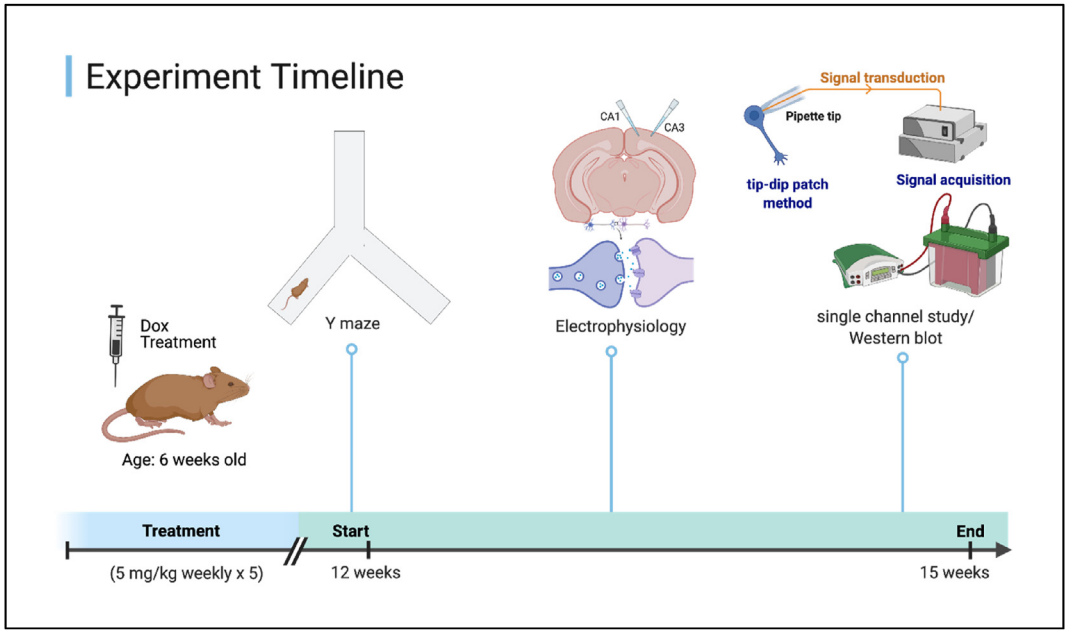

Figure 1. Experimental timeline. 6-week-old athymic male mice were treated with I.V tail vein injection of Dox (5 mg/kg) once weekly for 5 weeks. Y maze was performed at 12 weeks of age. A separate set of animals were utilized for electrophysiology (LTP), synaptosome preparation and western blot experiments. This figure is "Created with BioRender.com" (https://biorender.com/).

at which initial population spike appeared. LTP was induced by Theta Burst Stimulation (TBS) protocol after a stable baseline recording for 10–15 min. The TBS protocol contains 5 sweeps at an interval of 20s, and each sweep contains 10 bursts of stimuli. Each train contains four pulses at 100 Hz, with an inter-burst interval of 200 ms. The recording was continued for 60 min post-TBS (Bloemer et al., 2019; Govindarajulu et al., 2020). LTP was calculated as an average of fEPSP slopes from 50-60 min post induction. Sweep analysis was computed by normalizing the amplitude of the first fEPSP of sweep 2 to sweep 5 with the amplitude of the first fEPSP of the sweep 1. Field potentials were recorded using LTP software with Axoclamp 2B (Axon Instruments, Foster City, CA) and analyzed with Win software (Bristol, UK) (Anderson and Collingridge, 2007).

2.6. Synaptosome preparation

The synaptosomes were isolated as previously described (Johnson et al., 1997). Mice were euthanized with CO_2. Brains were removed and immersed into ice-cold oxygenated phosphate buffered saline (PBS) (95% O_2 and 5% CO_2). The hippocampus was dissected, submerged in oxygenated modified Krebs-Henseleit buffer (mKREBS) (118.5 mM NaCl, 4.7 mM KCl, 1.18 mM $MgSO_4$, 2.5 mM $CaCl_2$, 1.18 mM KH_2PO4, 24.9 mM $NaHCO_3$, 10 mM dextrose, 10mM adenosinede aminase, pH 7.4), and homogenized with a handheld Potter homogenizer. Samples were maintained at 4 °C on ice. Protease inhibitors (0.01 mg/ml leupeptin, 0.005 mg/ml pepstatin A, 0.10 mg/ml aprotinin, 5 mM Benzamide; Thermo Fisher scientific, Cat# 78436) were added to the homogenized buffer to diminish proteolysis. The homogenate was filtered through nylon filter (100 μm, obtained from BD Falcon, Bedford, MA) and a low-protein binding filter (5 μm, obtained from Millex-SV; Millipore Corp., Bedford, MA). Filtered homogenate was centrifuged at 1000g for 15 min at 4 °C. The supernatant was removed; the pellet (Synaptosome) was resuspended with 20 μl mKREBS and stored in -80 °C until use (Johnson et al., 1997; Parameshwaran et al., 2012; Vaithianathan et al., 2005).

2.7. Single channel recording

The single channel recording was performed as described previously (Hammond et al., 2006; Parameshwaran et al., 2013). 'Tip-dip" method was used to incorporate AMPARs from synaptosomal fractions in artificial lipid bilayers (Suppiramaniam et al., 2006). Briefly, preparation of the artificial lipid bilayer membrane was performed by evaporating chloroform from 1,2 diphytanoyl-sn-glycero-3-phosphocholine (Avanti Polar-Lipids Inc., Alabaster, AL) with a stream of nitrogen and then dissolving the precipitate with anhydrous hexane at 1 mg/ml concentration (Sigma-Aldrich Co., Milwaukee, WI). The glass electrode (1.5 mm diameter, 100 mΩ) was pulled to create a pipette with 1 μm diameter and then filled with intercellular fluids (ICF), composed of 110 mM KCl, 4 mM NaCl, 2 mM $NaHCO_3$, 1 mM $MgCl_2$, 0.1 mM $CaCl_2$, and 2 mM 3-N-Morpholino propane sulfonic acid with adjusted pH of 7.4. The pulled pipette was then placed with a reference electrode and immersed in a microbeaker containing extracellular fluid (ECF; 125 mM NaCl, 5 mM KCl, 1.25 mM NaH_2PO_4, and 5 mM Tris HCl solution, and adjusted to pH 7.4). Then 5 μl of the phospholipid was added to the ECF, which spreads out to form lipid monolayers on the top of the ECF. The bilayer was formed by successive transfer of two monolayers onto the tip of the patch pipette with "outside-out" configuration. After forming a stable membrane, 3–5 μL suspension of the synaptosomes was delivered to the bath solution. AMPA receptor single channel currents were evoked and isolated by adding AMPA (290 nM, Tocris 0169), tetrodotoxin (1 μM, Tocris 1078), tetraethyammonium chloride (2 μM, Tocris 3068), AP5 (50 μM, Tocris 0106), methyl glutamate analog (2S, 4R)-4-methylglutamate (SYM 2081; 1 μM, Tocris 0903), PTX (100 μM, Tocris 1128) and voltage clamped at +94 mV. Single channel currents were low-pass filtered (2 kHz), and digitized (5 kHz) (Mini-digi, Molecular Devices). Data was acquired with pClamp9 software (Molecular Devices), and saved on a computer for off-line analysis. Current amplitude histograms were constructed and fitted with Gaussian method to detect individual conductance levels. Single channel open probability was computed from areas under the current-amplitude histograms. Log transformed dwell time count histograms were constructed and fitted with variable metric method to identify distinct open and close times (Parameshwaran et al., 2007).

2.8. Immunoblot analysis

Following euthanasia, hippocampus was dissected and homogenized in lysis buffer (Neuronal Protein Extraction Reagent, Thermo Fischer Scientific). Halt Protease and phosphatase inhibitor cocktail (Thermo Fischer Scientific, cat# 78440) was also added to the lysis buffer. Total protein was assessed by BCA assay (Pierce BCA Protein Assay Kit, Thermo Fischer Scientific, Cat# 23225). Prepared hippocampal sample containing equal amount of protein (40μg) was loaded into 10% polyacrylamide gel. The proteins were then transferred to PVDF membranes (0.45 μm; Immobilon-p Millipore, Germany), and blocked with 5% non-fat dry milk for 1 h in Tris buffered saline containing 0.1% Tween 20 (TBST). Membranes were washed with TBST for 3 times5 minutes each and incubated in primary antibodies (Table 1) in 5% BSA overnight at 4 °C. Next day, membranes were probed with either secondary anti-mouse antibody (1:2,000) or anti-rabbit antibody (1:10,000) conjugated with fluorophore DyLight 550 at room temperature for 60–90 min. Membranes were scanned and visualized by FluorChem Q imager system and the density of immunoreactivity for each band was measured using Alpha-View software (Protein Simple) and values were normalized to the beta actin levels of corresponding lanes.

2.9. Statistics

Behavior in the Y maze was analyzed with a repeated measures analysis of variance (RMANOVA), using group and arm (Novel vs. Familiar [average of Known and Entry arms]) as factors, followed by planned comparisons. All scores were analyzed for outlier scores using Grubbs' test (Grubbs, 1969). One mouse in the Dox group was an outlier in its dwell time in both the Familiar and Novel ($Zs = 1.98$ and 2.03, respectively, critical value $= 1.89$) arms. All analyses were conducted excluding this subject. Because of the relatively small size of the groups ($n = 5$ to 6 per group), effect sizes are presented for all significant effects (partial eta squared [η_p^2], using the convention 0.01, 0.06, and 0.14 for small, medium, and large effects, respectively (Cohen, 1988). The fEPSP and single channel data were analyzed with WinLTP and pClamp 9 programs, respectively. Statistical analysis was performed using Prism software. Comparison of the two experimental groups, i.e., Control and Dox was performed by two-tailed, unpaired and paired Student t-tests, where appropriate. For all parametric statistics, results were considered significantly different when $p < 0.05$. All data are presented as mean ± SEM.

3. Results

3.1. Dox affects spatial memory in the Y-maze task

In the Y-maze, intact memory functioning should lead to an increased number of entries and potentially longer exploration time of the arm that was not visited during the training period (Novel arm). The Dox and control mice did not differ in number of total arm entries during testing, indicating similar levels of activity between groups (Figure 2B); that is, any further effects were not due to Dox reducing overall levels of activity in the treated animals. Entries into each arm of the Y-maze are related to the subjects' previous experience with the arm, with preference for the previously non-visited (Novel) arm. There was a main effect of group, as well as an interaction between group and

Table 1. Summary of antibodies and working conditions used in immunoblotting experiment.

Antibodies	Host & Type	specificity	Source	Cat#	RRID	Dilution
Primary Antibodies						
Anti-GAPDH	Rabbit, monoclonal	H M R Mk	Cell Signaling Technology	5174	AB_10622025	1:1,000
Anti- β-actin	Rabbit, monoclonal	H M R Mk Dm Z	Cell Signaling Technology	8457	AB_10950489	1:1,000
Anti-GluA1	Rabbit, monoclonal	M R	Cell Signaling Technology	13185	AB_2732897	1:1,000
Anti- phospho GluA1 Ser 845	Rabbit, monoclonal	H M R	Cell Signaling Technology	8084	AB_10860773	1:1,000
Anti- GluA2	Rabbit, monoclonal	H M R	Cell Signaling Technology	13607	AB_2650557	1:1,000
Anti-CaMKII	Rabbit, monoclonal	H M R	Cell Signaling Technology	11945	AB_2797775	1:1,000
Anti-phospho-CaMKII	Rabbit, monoclonal	H M R Dr	EMD Millipore	AB3865	AB_11212950	1:1,000
Anti-BDNF	mouse, monoclonal	H M R B Pg Dg	Santa Cruz	sc-546	AB_630940	1:1,000
Anti-α-stargazin	Rabbit, monoclonal	M R	EMD Millipore	AB9876	AB_877307	1:1,000
Anti-AKT	Rabbit, monoclonal	H M R Hm Mk C Dm B Dg Pg	Cell Signaling Technology	9272	AB_329827	1:1,000
Anti-phospho-AKT	Rabbit, monoclonal	H M R Hm Dm B Dg Pg	Cell Signaling Technology	9271	AB_329825	1:1,000
Anti-ERK	Rabbit, monoclonal	H M R Hm Mk Mi Dm Z B Dg Pg Ce	Cell Signaling Technology	4695	AB_390779	1:2,000
Anti-phospho-ERK	Rabbit, monoclonal	H M R Hm Mk Mi Dm Z B Dg Pg Sc	Cell Signaling Technology	4370	AB_2315112	1:1,000
Secondary Antibody						
Anti-rabbit IgG	Goat, polyclonal	R	Thermo Scientific	AB228334	AB_228334	1:10,000
Anti-mouse IgG	horseradish peroxidase, monoclonal	M	Santa Cruz	sc-516102	AB_2687626	1:2,000

H-Human, M-Mouse, R-Rat, Hm-Hamster, Mk-Monkey, Mi-Mink, C-Chicken, Dm-D. melanogaster, X-Xenopus, Z-Zebrafish, B-Bovine Dg-Dog, Pg-Pig, Sc-S. cerevisiae, Ce-C. elegans, Hr-Horse, Dr-Drosophila.

arm entered more frequently, with control mice making more entries into the Novel than the Familiar arms, whereas Dox-treated mice showed the opposite pattern (Figure 2C, $F_{1,9} = 16.43$, $p < 0.005$, $\eta_p^2 = 0.65$). The number of entries into the Novel arm was higher for the control than the Dox group ($F_{1,9} = 16.43$, $p < .005$). Furthermore, animals in the control group made more entries into the Novel than the Familiar arms ($F_{1,9} = 8.16$, $p < .05$), whereas animals in the Dox group made more entries into the Familiar than the Novel arms ($F_{1,9} = 8.30$, $p < .05$). The lack of preference for the Novel arm observed in the Dox-treated animals seems to reflect a deficit in reference spatial memory, as there were no differences in number of alternations (working spatial memory) between the Dox-treated and control animals (Figure 2D). An analysis of dwell time, which provides a measure of exploratory behavior, yielded a main effect of group and an interaction between group and arm that mirrored the pattern observed with number of entries (Figure 2E; $F_{1,9} = 5.89$, $p < .05$, $\eta_p^2 = 0.40$). Control animals spent more time in the Novel arm than the Dox-treated animals ($F_{1,9} = 5.88$, $p < .05$). Control animals spent more time in the Novel arm than the

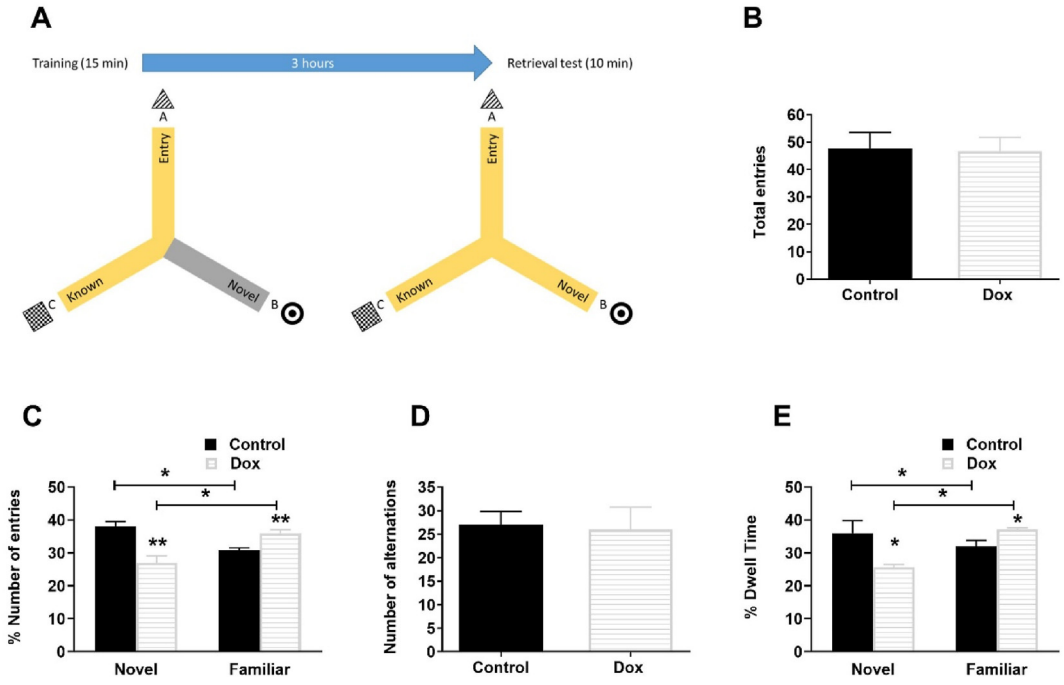

Figure 2. Dox treated mice displayed deficits in spatial memory assessed with the Y-maze. (A) Schematic representation of the Y -maze procedure. (B) Total number of arm entries during testing revealed no differences in overall activity. (C) percentage of entries into the Novel arm during testing revealed a decreased response to novelty in Dox-treated animals, and a significant treatment x arm interaction. (D) Number of alternations revealed no deficits in spatial working memory. (E) Percent time spent in novel arm during testing revealed attenuated exploratory behavior in Dox-treated animals, and a significant treatment x arm interaction. Bars represent mean ± SEM; *p < .05, **p < 0.005; n = 5 animals in Dox group and 6 animals in control group.

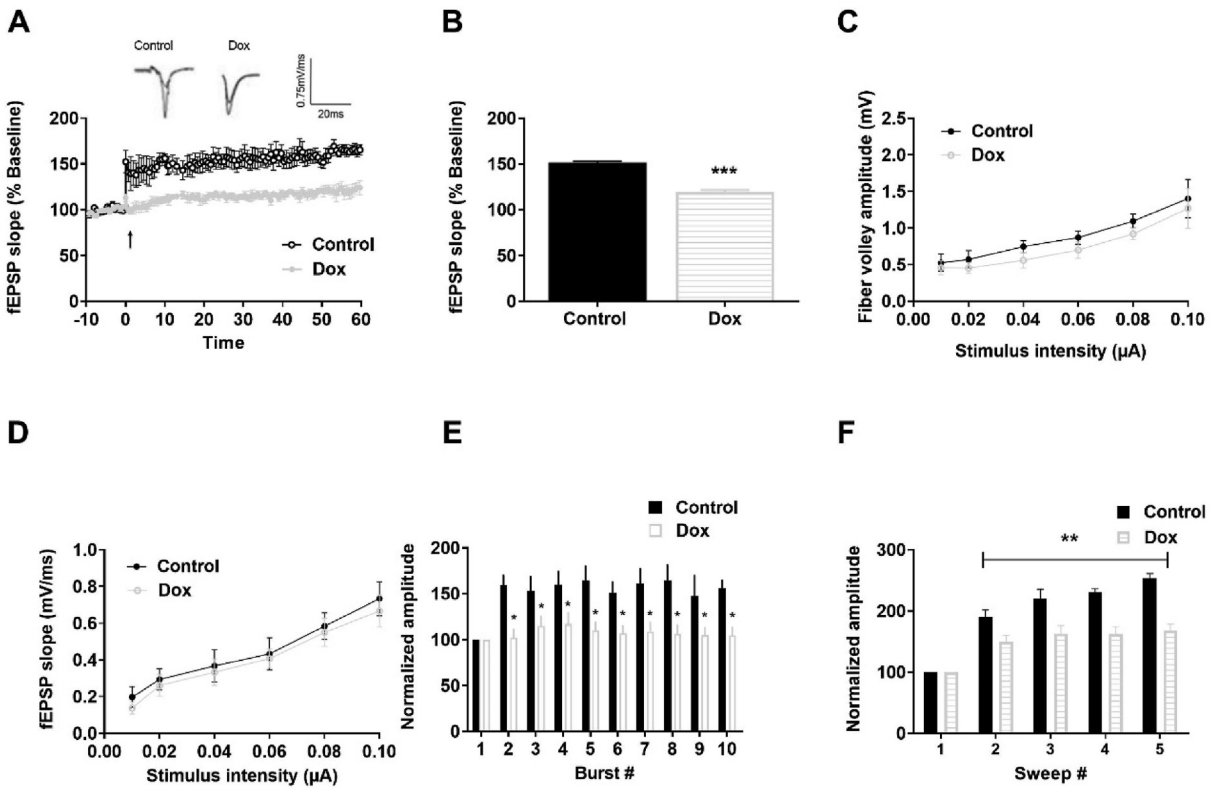

Figure 3. Dox-treated mice display a reduction in LTP. (A) LTP graph representing fEPSP slope before and after induction, as indicated by arrow. Mean slope of fEPSPs recorded 10 min prior to TBS was taken as 100%. (B) LTP bar graph showing fEPSPs recorded for 50–60 min post TBS induction and normalized to baselines levels. (C) Input-output curve depicting the FV amplitude across a range of increasing stimulus intensities. (D) Input output curve depicting fEPSP slope across a range of stimulus intensities. (E) Within-train facilitation, facilitation of the fEPSPs within individual TBS, was computed by normalizing the amplitude of fEPSPs #2–10 with the amplitude of the first fEPSP. (F) Sweep analysis calculated by normalizing the amplitude of the first fEPSP of sweeps 2–5 with the amplitude of the first fEPSP of sweep 1. Symbols/Bars represent mean ± SEM; *indicates significant difference between Control and Dox-treated mice, *p < 0.05, **p < 0.01, ***p < .001; n = 5–6 slices from 4 mice per group; Two tailed Student's t-test.

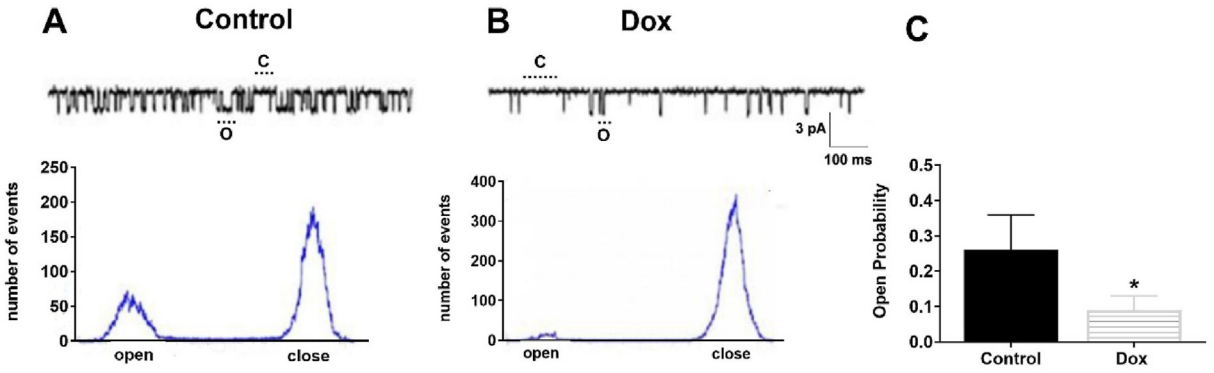

Figure 4. Dox treatment altered the single-channel properties of hippocampal synaptic AMPA receptors. (A–B) Amplitude histograms display two distinct peaks for close (c) and open (o) states. Channel open peak is higher in the control than Dox-treated mice. (C) Bar chart illustrating the significant reduction of AMPA receptors channel open probability in the Dox-treated group. Bars represent mean ± SEM, *indicates significant difference between Control and Dox-treated mice, *p < 0.05, n = 6 mice per group; Two tailed Student's t-test.

Familiar arms ($F_{1,9} = 5.93$, $p < .05$), but time spent in both arms was equivalent in the Dox treated group.

3.2. Dox treatment impairs long-term potentiation without altering presynaptic release probability

To assess whether the behavioral deficits in Dox-treated mice coincide with alterations in synaptic plasticity, we measured LTP in acute hippocampal slices (Figure 3A). Dox-treated mice displayed LTP deficits in the Schaeffer collateral pathway compared to control mice (Figure 3B, mean ± SEM for control 151 ± 1.49 and Dox 119.25 ± 2.17, p < 0.001). To determine whether the reduction in LTP was associated with presynaptic changes, we assessed the fiber volley (FV) amplitude, which denotes presynaptic axonal recruitment. We did not observe any significant changes in the FV amplitude between the groups (Figure 3C) suggesting that the change in the LTP may be not due to alterations in presynaptic axonal recruitment. Next, we examined changes in the slope of fEPSP across a range of stimuli, which indicates alterations in basal

Table 2. Single channel properties of synaptic AMPA receptors in the control and Dox-treated mice.

	Control (±SEM)	Dox (±SEM)
Open time (ms)		
τO_1	7.36 ± 1.46	1.23 ± 0.23*
τO_2	240.7 ± 12.35	160.93 ± 17.01**
Close time (ms)		
τC_1	0.21 ± .026	0.43 ± 0.037*
τC_2	216.15 ± 24.97	524.02 ± 18.23*

Data represent mean ± SEM, *indicates significant difference between Control and Dox-treated mice, *$p < 0.05$, **$p < 0.01$, n = 6 mice per group; Two tailed Student's t-test.

synaptic transmission. No difference in basal synaptic transmission was observed between control and Dox-treated mice (Figure 3D). The reduction in LTP in the Dox-treated mice could indicate alterations in the strength of the signaling through postsynaptic receptors during LTP induction or maintenance. To assess for alterations in LTP induction, we evaluated fEPSP amplitude during TBS induction and observed an increase in fEPSP induction of approximately 15–20% from baseline in Dox-treated mice, whereas the increase in control mice was approximately 70–80% from baseline (Figure 3E, $p < 0.05$). When amplitudes of the fEPSPs elicited within each sweep were normalized to the first fEPSP, a significant reduction was observed in the fEPSP amplitude in the Dox-treated mice (mean ± SEM = 134.00 ± 5.78) compared to control mice (mean ± SEM = 285.5 ± 30.4) (Figure 3F, $p < 0.01$), implying that the LTP impairment could be possibly due to reduced synaptic activation during LTP induction.

3.3. Effects of dox treatment on single-channel properties of synaptosomal AMPA receptors

Since LTP maintenance is highly dependent on AMPAR function (Chater and Goda, 2014), we further investigated whether LTP deficits in Dox-treated mice were associated with alterations in synaptic AMPAR function. Therefore, in the next set of experiments, synaptic AMPAR mediated single-channel currents were recorded by utilizing hippocampal synaptosomes as described elsewhere (Parameshwaran et al., 2013) to investigate whether Dox treatment resulted in alteration in AMPAR channel properties. Single channel recordings showed that Dox treatment alters synaptic AMPAR function. The current amplitude histograms showed a significant decrease in the frequency of single channel probability of opening as indicated by the area under the curve in the Dox treatment group (Figure 4B) compared to control (Figure 4A). The probability of opening of AMPAR channel (P_o) was significantly decreased in Dox-treated mice (mean ± SEM = 0.09 ± .02) compared to control mice (mean ± SEM = 0.26 ± .06) (Figure 4C, $p < .05$). In addition, the dwell-open times showed a marked decrease in dwell open times along with a significant increase in dwell closed times of AMPAR channels in the Dox-treated mice compared to control mice (Table 2).

3.4. Dox treatment results in altered phosphorylation of AMPAR subunits in the hippocampus

Since we observed change in AMPAR function, we next explored the relative levels of AMPAR subunits and key downstream signaling proteins required for AMPAR trafficking during LTP in the hippocampus. Our results illustrate that Dox treatment produced a robust decrease in GluA1 level (Figure 5A, $p < 0.05$) but an increase GluA2 level (Figure5B, $p < 0.05$) in the hippocampus. Since, GluA2 knockout mouse model exhibit enhanced LTP (Jia et al., 1996) an increase in the GluA2 may be linked to the LTP deficits in Dox-treated mice. A major phosphorylation site of GluA1 that impact synaptic plasticity is Ser845, which occurs in the C-terminus of GluA1 (Gray et al., 2014). Dox treatment reduced Ser845 phosphorylation of GluA1 (Figure 5C, $p < 0.05$), which can enhance synaptic plasticity and memory function by increasing the probability of channel opening. Since we observed a reduction in AMPAR channel opening in the Dox-treated mice, this may be due to the reduction in GluA1 Ser845 phosphorylation. Our results illustrate that Dox treatment leads to changes in synaptic strength, likely via functional alterations in AMPARs.

3.5. Dox treatment alters AMPAR downstream signaling proteins in the hippocampus

Since we observed a change in the AMPAR subunit levels, next we examined the downstream signaling molecules of AMPAR. Phosphorylation of CaMKII was reduced in Dox-treated mice (Figure 6A, $p < 0.05$). CaMKII plays an essential role in the trafficking and insertion of AMPARs to the membrane increases postsynaptic response to presynaptic depolarization through synaptic strengthening. Transmembrane AMPAR regulatory protein (TARP) γ2 or stargazin is an AMPAR auxiliary subunit is necessary for efficient diffusion of AMPARs to the synaptic surface (Bissen et al., 2019b). A reduction in the level of α-stargazin was observed in the hippocampi of Dox-treated mice (Figure 6B, $p < 0.05$). Brain -derived neurotrophic factor (BDNF), a major mediator of LTP, was

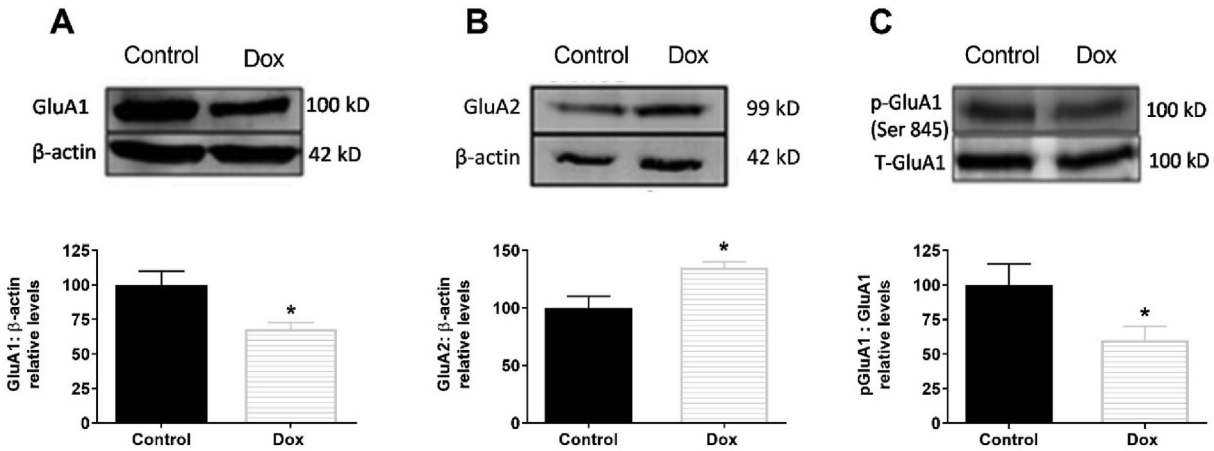

Figure 5. Dox treatment results in alterations glutamate receptor proteins' level. Representative immunoblot showing (A) GluA1 (B) GluA2 (C) p-GluA1 Ser845 relative levels normalized to beta-actin. Bars represent mean ± SEM; *indicates significant difference between Control and Dox-treated mice, *$p < 0.05$, **$p < 0.01$; n = 3–4 mice per group; Two tailed Student's t-test.

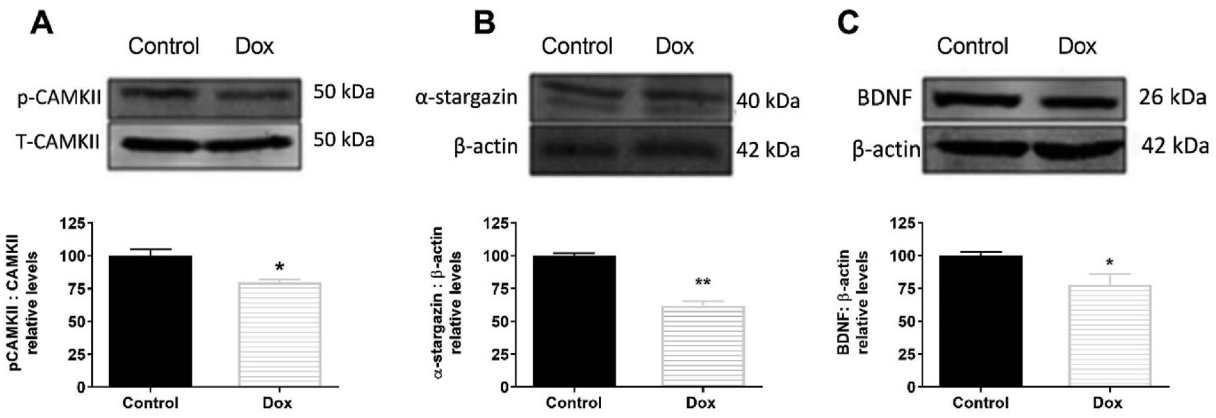

Figure 6. Dox treatment causes an alteration in the synaptic proteins' level. Representative immunoblot showing (A) p-CaMKII (B) α-stargazin (C) BDNF relative levels normalized to beta-actin. Bars represent mean ± SEM; *indicates significant difference between control and Dox-treated mice, *p < 0.05, **p < 0.01 n = 3–4 mice per group; Two tailed Student's t-test.

also reduced in the Dox-treated mice (Figure 6C, $p < 0.05$). Thus, LTP deficits may be due to alterations in AMPAR trafficking and function associated with a reduction in CaMKII phosphorylation.

3.6. Dox treatment alters expression of proteins that are important for neurogenesis and synaptic plasticity

There are several other proteins that are vital for maintenance of synaptic plasticity. Since we observed a deficit in LTP, we investigated the expression of downstream proteins crucial for maintaining stable synaptic plasticity. We previously found that acute Dox treatment in hippocampal cells resulted in altered activation of key proteins such as AKT, ERK and p38 (Alhowail et al., 2019). In the current study, we observed that behavioral and synaptic plasticity deficits in Dox-treated mice were also accompanied by an increased phosphorylation of ERK (Figure 7A, $p < 0.05$) and AKT (Figure7B, $p < 0.01$). Thus, it can be suggested that the observed hippocampal deficits are associated with altered ERK-AKT signaling.

4. Discussion

In this study, we used an athymic, nude mouse model of Dox-induced cognitive impairment and hypothesized that Dox treatment would cause deficits in hippocampal synaptic plasticity and consequently, spatial memory, via impairment of LTP, alterations in postsynaptic AMPAR expression and function, and associated dysregulation of downstream signaling (Figure 8). The observed reduction in GluA1 levels and alterations in single channels AMPAR properties indicate dysfunction of AMPAR signaling following exposure to Dox. Previously, we elucidated the neurotoxic effects and mechanisms of Dox on spatial memory and the hippocampal glutamatergic system associated with the cognitive impairment (Alhowail et al., 2019). To the best of our knowledge, this is the first study that demonstrated the effect of Dox on synaptic hippocampal AMPARs, thus identifying a novel pathology that may explain some of the cognitive deficits observed in individuals receiving Dox chemotherapy.

In the Y-maze task, mice treated with Dox did not differ from control mice in overall exploratory behavior indicating that Dox did not increase

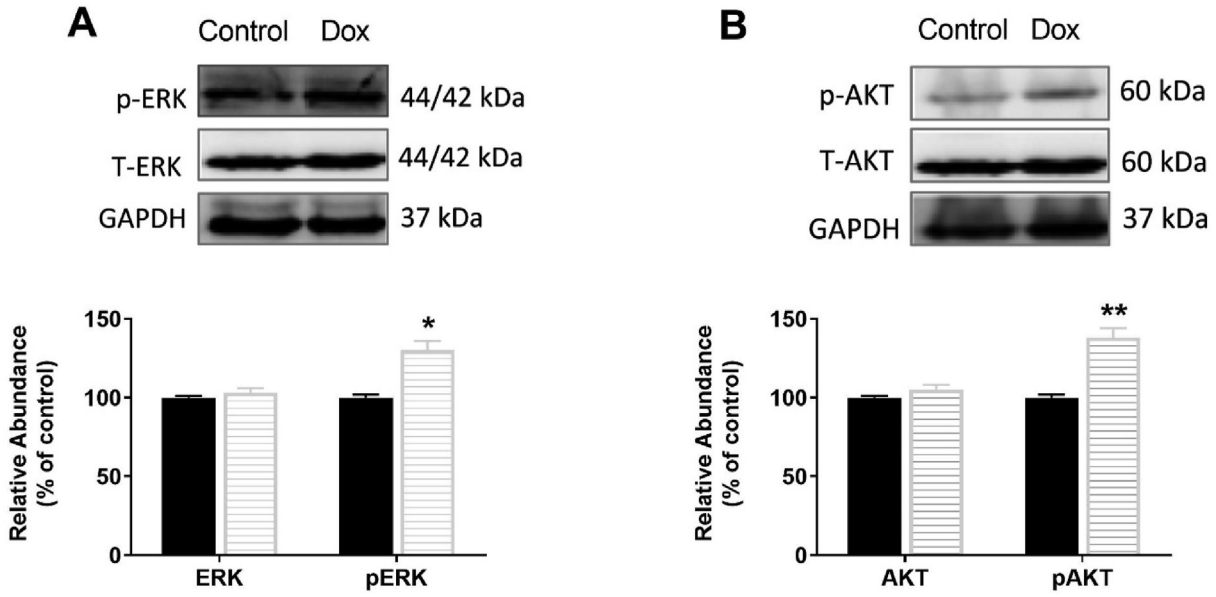

Figure 7. Dox treatment alters expressions of proteins required for neurogenesis and synaptic plasticity. Representative immunoblot showing (A) p-ERK/ERK and ERK/GAPDH (B) p-AKT/AKT and AKT/GAPDH levels in the total hippocampal lysate. Bars represent mean ± SEM; *indicates significant difference between Control and Dox-treated mice, *p < 0.05, **p < 0.01 n = 3–4 mice per group; Two tailed Student's t-test.

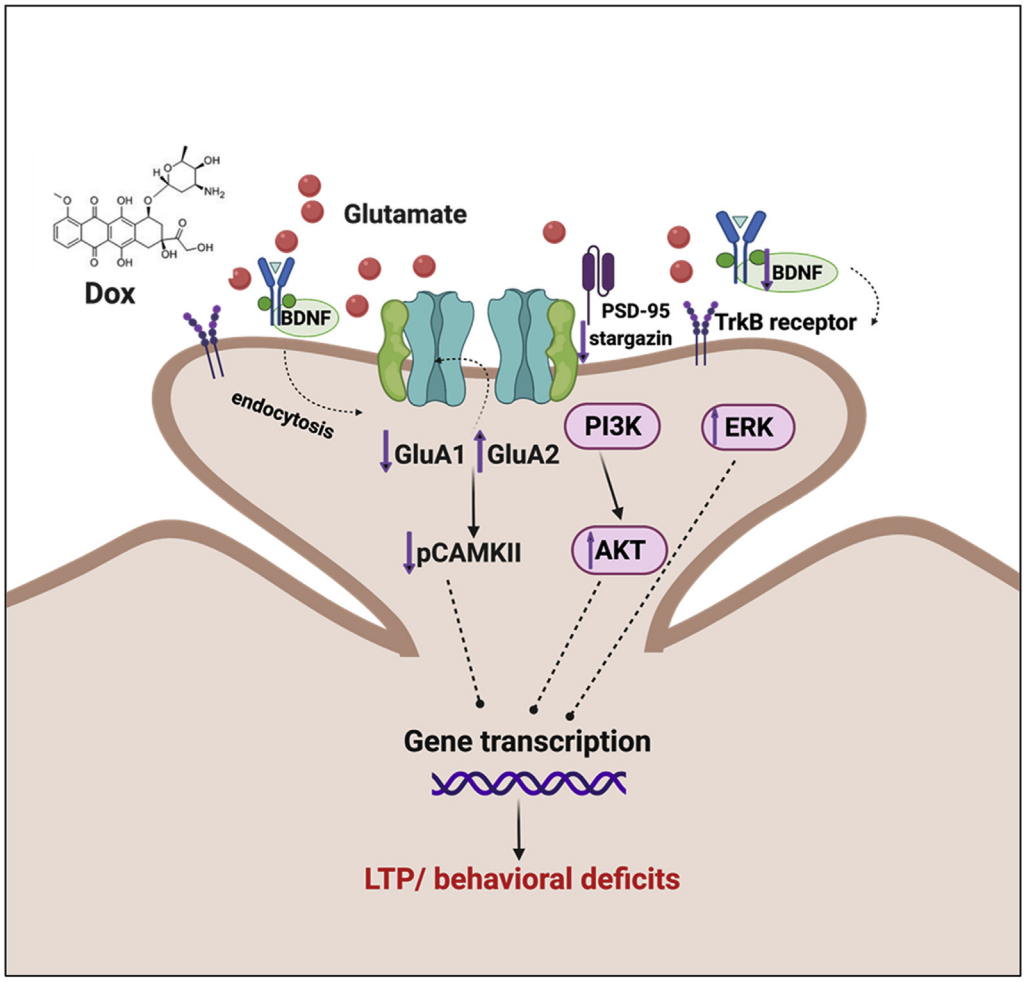

Figure 8. Dox mediated impairment in synaptic plasticity. Dox treatment in mice decreases GluA1R and increases GluA2R level causing a reduction in CAMKII phosphorylation. A reduction in α-stargazin is also present affecting AMPAR trafficking through its interaction with PSD-95. Furthermore, Dox also causes a reduction in BDNF leading to reduced trafficking and insertion of GluA1 into the post synaptic membrane. Increased phosphorylation of ERK and AKT along with possible alterations in their upstream protein PI3K have been observed. These alterations in the synaptic plasticity proteins altogether leads to LTP and behavioral deficits in the mice. Dox- Doxorubicin; BDNF- Brain derived neurotrophic factor; CAMKII- Ca2+/calmodulin-dependent protein kinase II; ERK-Extracellular Regulated Kinase; AKT- Protein Kinase B; LTP- Long-term potentiation; This figure is "Created with BioRender.com" (https://biorender.com/).

general anxiety or neophobia. Dox treatment did not appear to affect working memory, as evidenced by a lack of differences in spontaneous alternations between the Dox and control subjects. However, Dox treatment appeared to significantly impair long-term, reference memory. Dox-treated animals made fewer entries and spent less time in the Novel than the Familiar arms, suggesting that they failed to recognize the novelty of the previously unexplored arm. Similar observations have also been reported after treatment with other chemotherapeutic agents (Konat et al., 2008; Salas-Ramirez et al., 2015). In Dox-treated mice, a significant deficit in LTP was observed. LTP is a type of long-term synaptic plasticity which provides a cellular and molecular correlations by which memories are formed (Citri and Malenka, 2008). The induction phase of LTP in the hippocampal schaffer collateral pathway is predominantly NMDAR dependent while the maintenance phase is predominantly AMPAR dependent (Malenka and Nicoll, 1993; Malinow and Malenka, 2002). The observed LTP deficits in the Dox-treated mice could be either due to presynaptic or postsynaptic alterations. However, no significant difference in presynaptic axonal recruitment as indicated by PPF was observed between control and Dox-treated mice suggesting that the LTP deficits observed in this study may be primarily due to postsynaptic alterations.

Two AMPAR subunits that play significant roles in learning and memory are GluA1 and GluA2. However, they are different in their permeability to Ca^{2+}. GluA1 subunits are permeable to Ca^{2+}, whereas the edited version of GluA2 is Ca^{2+} impermeable (Geiger et al., 1995; Ozawa, 2009). Ca^{2+} influx into the postsynaptic neuron is necessary for the LTP through the activation of CaMKII. We observed an increase GluA2, and a reduction in GluA1 in the Dox-treated mice as well as a reduction in the phosphorylation of CaMKII which might be due to decreased Ca^{2+} influx through AMPARs (Meng et al., 2003). Phosphorylation of amino acid residues within the GluA1 subunit are modified during LTP (Chater and Goda, 2014; Diering et al., 2016; Lee, 2006). Our results indicate decreased phosphorylation of GluA1 Ser845 which is essential to promote GluA1 cell-surface insertion and synaptic retention, increases the opening probability, and to facilitate the induction of LTP (He et al., 2009; Henley and Wilkinson, 2013; Oh et al., 2006). In congruence with that, we have also observed a reduction in the single channel opening probability of AMPAR in synaptosomes from Dox-treated mice. A decrease in open probability reduces the mean current amplitude of the single ion channel, resulting in decreased postsynaptic potentials and consequently, a reduced likelihood of LTP at that synapse leading to cognitive dysfunction (Béïque et al., 2006). A decrease in single channel conductance of synaptic AMPAR was also observed in synaptosomes extracted from Dox-treated group. Thus, the synaptic plasticity deficits might be due to AMPAR mediated reduction in the postsynaptic currents due to antagonizing actions of Dox or its metabolites on AMPAR. It could be also due to increased desensitization of AMPAR in response to Dox treatment as indicated by decrease in opening events. Furthermore, alterations in AMPAR dependent downstream signaling cascades may also lead to synaptic plasticity deficits. The transmembrane protein α-stargazin interacts with AMPARs to facilitate AMPAR trafficking and enhance surface expression of AMPARs (Deng et al., 2006). Stargazin can also directly regulate AMPAR channel properties by increasing the opening probability (Tomita et al., 2005). In the present study, α-stargazin is downregulated following Dox treatment, which may contribute to the reduction in AMPAR opening probability. Since Dox can also affect neurogenesis (Inagaki et al., 2007; Kitamura et al., 2015); we next

explored a key regulatory protein of the neurogenesis pathway as another potential mechanism for chemotherapy-induced memory impairment. BDNF is a known contributor of synaptic transmission and synaptic plasticity in the hippocampus (Cunha et al., 2010; De Vincenti et al., 2019). BDNF activates CaMKII and regulates AMPAR trafficking through interactions with α-stargazin (Nakata and Nakamura, 2007; Zhang et al., 2018). The reduction in BDNF along with a reduction in α-stargazin in our study indicates that reduced AMPAR insertion in postsynaptic density may contribute to the LTP impairments in Dox-treated mice. Thus we suggest that decreased trafficking of AMPARs to the synapses and decreased single channel open probability related to a downregulation of α-stargazin and BDNF may contribute to the LTP deficits leading to memory impairment.

Moreover, proper AKT and ERK signaling are required for normal neuronal development, function, and synaptic plasticity (Alonso et al., 2004; Easton et al., 2005). Previously, we have observed an increase in ERK and AKT activation following acute *in vitro* exposure to Dox (Alhowail et al., 2019). In congruence with that, prolonged exposure to Dox in the current *in vivo* study also increased ERK and AKT phosphorylation. The increase in ERK phosphorylation could be due to a decrease MKP-1 (MAPK phosphatase-1) expression or delayed MEK (Mitogen-activated protein kinase kinase) activation (Lakshminarasimhan et al., 2017). An increase in MAPK/ERK activation could be also associated with chemoresistance. ERK activation can protect cells from Dox induced cell death and promote Dox resistance by activating MAPK/ERK pathway and/or JNK/p38 pathways in response to increased ROS production (Christowitz et al., 2019; McCubrey et al., 2007). The increase in AKT phosphorylation may be also due over production of ROS following Dox treatment (Ahn et al., 2013; Barrera, 2012; Thorn et al., 2011) rather than direct effect of Dox. Similar to ERK, an increase in AKT activation is associated with chemoresistance (Li et al., 2005). Although a reduction in LTP is usually accompanied by a reduction in AKT phosphorylation (Levenga et al., 2017), strong AKT activation can in turn increase oxidative stress, cell death, and oncogenic senescence (Nogueira et al., 2008). However, a detailed investigation on the expression levels of upstream and downstream signaling proteins such as PI3K, p38MAPK, JNK, CREB, and various apoptotic proteins is warranted to fully elucidate Dox mediated alterations in ERK and AKT.

In summary, findings from our study support the hypothesis that Dox treatment leads to cognitive dysfunction. In addition, the present study has probed molecular mechanisms underlying Dox associated memory dysfunction by uncovering a possible link between chemobrain and alterations in the cellular machinery responsible for LTP. Our data suggest that Dox decreases AMPAR function and associated downstream protein signaling which results in impaired synaptic plasticity and spatial memory performance. Based on these findings, one therapeutic approach in the treatment of chemotherapy induced cognitive dysfunction may be to utilize AMPAR agonists or ampakines, which can increase cognition and LTP significantly in animal models (Lynch, 2002; Lynch and Gall, 2006). Interestingly, ampakines can also induce cell death in cancer cells exerting an oncolytic effect (Radin et al., 2018a, 2018b). However, the potential for beneficial effects of ampakines for the treatment of chemobrain needs to be validated clinically. Additionally, future studies are required to investigate whether NMDAR expression and functionality are also altered following Dox exposure. A thorough understanding of mechanisms responsible for chemobrain can pave the way for pharmacological interventions to mitigate the cognitive impacts of chemotherapeutics.

Declarations

Author contribution statement

Ahmad H. Alhowail: Conceived and designed the experiments; Performed the experiments; Analyzed and interpreted the data; Wrote the paper.

Priyanka D. Pinky: Conceived and designed the experiments; Performed the experiments; Analyzed and interpreted the data; Wrote the paper.

Matthew Eggert: Conceived and designed the experiments; Performed the experiments; Analyzed and interpreted the data.

Jenna Bloemer; Lauren N. Woodie; Manal A. Buabeid; Subhrajit Bhattacharya; Shanese L. Jasper; Dwipayan Bhattacharya: Performed the experiments; Analyzed and interpreted the data.

Muralikrishnan Dhanasekaran: Conceived and designed the experiments.

Martha Escobar: Conceived and designed the experiments; Performed the experiments; Analyzed and interpreted the data.

Robert D. Arnold; Vishnu Suppiramaniam: Conceived and designed the experiments; Analyzed and interpreted the data.

Funding statement

This work was supported by Auburn University (AU) Research Initiative in Cancer under an intramural grant titled 'Elucidation of Molecular Mechanisms of Chemobrain: Identification of Targets and Therapies' (Suppiramaniam/Arnold).

Data availability statement

Data will be made available on request.

Declaration of interests statement

The authors declare no conflict of interest.

Additional information

No additional information is available for this paper.

Acknowledgements

We would like to thank the Auburn University Research Initiative in Cancer (AURIC) and Auburn university Specialized Pharmaceutical and Experimental Center for Translational Research and Analysis.

References

Aguayo, F.I., Tejos-Bravo, M., Díaz-Véliz, G., Pacheco, A., García-Rojo, G., Corrales, W., Olave, F.A., Aliaga, E., Ulloa, J.L., Avalos, A.M., Román-Albasini, L., Rojas, P.S., Fiedler, J.L., 2018. Hippocampal memory recovery after acute stress: a behavioral, morphological and molecular study. Front. Mol. Neurosci. 11, 283.

Ahles, T.A., Saykin, A.J., 2007. Candidate mechanisms for chemotherapy-induced cognitive changes. Nat. Rev. Cancer.

Ahn, S., Seo, E., Kim, K., Lee, S.J., 2013. Controlled cellular uptake and drug efficacy of nanotherapeutics. Sci. Rep. 3, 1–10.

Alhowail, A.H., Bloemer, J., Majrashi, M., Pinky, P.D., Bhattacharya, S., Yongli, Z., Bhattacharya, D., Eggert, M., Woodie, L., Buabeid, M.A., Johnson, N., Broadwater, A., Smith, B., Dhanasekaran, M., Arnold, R.D., Suppiramaniam, V., 2019. Doxorubicin-induced neurotoxicity is associated with acute alterations in synaptic plasticity, apoptosis, and lipid peroxidation. Toxicol. Mech. Methods 29, 457–466.

Alonso, M., Medina, J.H., Pozzo-Miller, L., 2004. ERK1/2 activation is necessary for BDNF to increase dendritic spine density in hippocampal CA1 pyramidal neurons. Learn. Mem. 11, 172–178.

Aluise, C.D., Sultana, R., Tangpong, J., Vore, M., St. Clair, D., Moscow, J.A., Butterfield, D.A., 2010. Chemo Brain (Chemo Fog) as a potential side effect of doxorubicin administration: role of cytokine-induced, oxidative/nitrosative stress in cognitive dysfunction. Adv. Exp. Med. Biol. 678, 147–156.

Anderson, W.W., Collingridge, G.L., 2007. Capabilities of the WinLTP data acquisition program extending beyond basic LTP experimental functions. J. Neurosci. Methods 162, 346–356.

Antkiewicz-Michaluk, L., Krzemieniecki, K., Romanska, I., Michaluk, J., Krygowska-Wajs, A., 2016. Acute treatment with doxorubicin induced neurochemical impairment of the function of dopamine system in rat brain structures. Pharmacol. Rep. 68, 627–630.

Arnold, R.D., Slack, J.E., Straubinger, R.M., 2004. Quantification of Doxorubicin and metabolites in rat plasma and small volume tissue samples by liquid chromatography/electrospray tandem mass spectroscopy. J. Chromatogr. B Anal. Technol. Biomed. Life Sci. 808, 141–152.

Arnold, R.D., Mager, D.E., Slack, J.E., Straubinger, R.M., 2005. Effect of repetitive administration of doxorubicin-containing liposomes on plasma pharmacokinetics and drug biodistribution in a rat brain tumor model. Clin. Cancer Res. 11, 8856–8865.
Bannerman, D.M., Sprengel, R., Sanderson, D.J., McHugh, S.B., Nicholas Rawlins, J.P., Monyer, H., Seeburg, P.H., 2014. Hippocampal Synaptic Plasticity, Spatial Memory and Anxiety.
Barrera, G., 2012. Oxidative stress and lipid peroxidation products in cancer progression and therapy. ISRN Oncol. 2012, 137289.
Béïque, J.C., Lin, D.T., Kang, M.G., Aizawa, H., Takamiya, K., Huganir, R.L., 2006. Synapse-specific regulation of AMPA receptor function by PSD-95. Proc. Natl. Acad. Sci. U. S. A. 103, 19535–19540.
Bhattacharya, S., Ma, Y., Dunn, A.R., Bradner, J.M., Scimemi, A., Miller, G.W., Traynelis, S.F., Wichmann, T., 2018. NMDA receptor blockade ameliorates abnormalities of spike firing of subthalamic nucleus neurons in a parkinsonian nonhuman primate. J. Neurosci. Res. 96, 1324–1335.
Bissen, D., Foss, F., Acker-Palmer, A., 2019a. AMPA receptors and their minions: auxiliary proteins in AMPA receptor trafficking. Cell. Mol. Life Sci.
Bissen, D., Foss, F., Acker-Palmer, A., 2019b. AMPA receptors and their minions: auxiliary proteins in AMPA receptor trafficking. Cell. Mol. Life Sci.
Bloemer, J., Pinky, P.D., Smith, W.D., Bhattacharya, D., Chauhan, A., Govindarajulu, M., Hong, H., Dhanasekaran, M., Judd, R., Amin, R.H., Reed, M.N., Suppiramaniam, V., 2019. Adiponectin knockout mice display cognitive and synaptic deficits. Front. Endocrinol. (Lausanne) 10.
Bodley, A., Liu, L.F., Israel, M., Seshadri, R., Koseki, Y., Giuliani, F.C., Kirschenbaum, S., Silber, R., Potmesil2, M., 1989. DNA Topoisomerase II-Mediated Interaction of Doxorubicin and Daunorubicin Congeners with DNA1.
Briones, T.L., Woods, J., 2011a. Chemotherapy-induced cognitive impairment is associated with decreases in cell proliferation and histone modifications. BMC Neurosci. 12.
Briones, T.L., Woods, J., 2011b. Chemotherapy-induced cognitive impairment is associated with decreases in cell proliferation and histone modifications. BMC Neurosci. 12, 124.
Chater, T.E., Goda, Y., 2014. The role of AMPA receptors in postsynaptic mechanisms of synaptic plasticity. Front. Cell. Neurosci.
Chen, L., Chetkovich, D.M., Petralia, R.S., Sweeney, N.T., Kawasaki, Y., Wenthold, R.J., Bredt, D.S., Nicoll, R.A., 2000. Stargazin regulates synaptic targeting of AMPA receptors by two distinct mechanisms. Nature 408, 936–943.
Christie, L.A., Acharya, M.M., Parihar, V.K., Nguyen, A., Martirosian, V., Limoli, C.L., 2012. Impaired cognitive function and hippocampal neurogenesis following cancer chemotherapy. Clin. Cancer Res. 18, 1954–1965.
Christowitz, C., Davis, T., Isaacs, A., Van Niekerk, G., Hattingh, S., Engelbrecht, A.M., 2019. Mechanisms of doxorubicin-induced drug resistance and drug resistant tumour growth in a murine breast tumour model. BMC Cancer 19, 1–10.
Citri, A., Malenka, R.C., 2008. Synaptic plasticity: multiple forms, functions, and mechanisms. Neuropsychopharmacology.
Cohen, J., 1988. Statistical Power Analysis for the Behavioral Sciences, Statistical Power Analysis for the Behavioral Sciences. Routledge.
Conrad, C.D., Galea, L.A.M., Kuroda, Y., McEwen, B.S., 1996. Chronic stress impairs rat spatial memory on the Y maze, and this effect is blocked by tianeptine treatment. Behav. Neurosci. 110, 1321–1334.
Cunha, C., Brambilla, R., Thomas, K.L., 2010. A simple role for BDNF in learning and memory? Front. Mol. Neurosci. 3, 1.
Damodar, G., Smitha, T., Gopinath, S., Vijayakumar, S., Rao, Y., 2014. An evaluation of hepatotoxicity in breast cancer patients receiving injection doxorubicin. Ann. Med. Health Sci. Res. 4, 74.
De Vincenti, A.P., Ríos, A.S., Paratcha, G., Ledda, F., 2019. Mechanisms that modulate and diversify BDNF functions: implications for hippocampal synaptic plasticity. Front. Cell. Neurosci. 13, 135.
Deng, W., Yue, Q., Rosenberg, P.A., Volpe, J.J., Jensen, F.E., 2006. Oligodendrocyte excitotoxicity determined by local glutamate accumulation and mitochondrial function. J. Neurochem. 98, 213–222.
Diering, G.H., Heo, S., Hussain, N.K., Liu, B., Huganir, R.L., 2016. Extensive phosphorylation of AMPA receptors in neurons. Proc. Natl. Acad. Sci. U. S. A. 113, E4920–E4927.
Easton, R.M., Cho, H., Roovers, K., Shineman, D.W., Mizrahi, M., Forman, M.S., Lee, V.M.-Y., Szabolcs, M., de Jong, R., Oltersdorf, T., Ludwig, T., Efstratiadis, A., Birnbaum, M.J., 2005. Role for Akt3/protein kinase Bgamma in attainment of normal brain size. Mol. Cell Biol. 25, 1869–1878.
Fink, C.C., Meyer, T., 2002. Molecular mechanisms of CaMKII activation in neuronal plasticity. Curr. Opin. Neurobiol. 12, 293–299.
Geiger, J.R.P., Melcher, T., Koh, D.S., Sakmann, B., Seeburg, P.H., Jonas, P., Monyer, H., 1995. Relative abundance of subunit mRNAs determines gating and Ca2+ permeability of AMPA receptors in principal neurons and interneurons in rat CNS. Neuron 15, 193–204.
Glutamate receptors, 2020. Centre for Synaptic Plasticity. University of Bristol [WWW Document]. URL. http://www.bristol.ac.uk/synaptic/receptors/. (Accessed 15 April 2020).
Govindarajulu, M., Pinky, P.D., Steinke, I., Bloemer, J., Ramesh, S., Kariharan, T., Rella, R.T., Bhattacharya, S., Dhanasekaran, M., Suppiramaniam, V., Amin, R.H., 2020. Gut metabolite TMAO induces synaptic plasticity deficits by promoting endoplasmic reticulum stress. Front. Mol. Neurosci. 13, 138.
Gray, E.E., Guglietta, R., Khakh, B.S., O'Dell, T.J., 2014. Inhibitory interactions between phosphorylation sites in the C terminus of α-Amino-3-hydroxy-5-methyl-4-isoxazolepropionic acid-type glutamate receptor GluA1 subunits. J. Biol. Chem. 289, 14600–14611.
Grubbs, F.E., 1969. Procedures for detecting outlying observations in samples. Technometrics 11, 1–21.
Hammond, M.S.L., Sims, C., Parameshwaran, K., Suppiramaniam, V., Schachner, M., Dityatev, A., 2006. Neural cell adhesion molecule-associated polysialic acid inhibits NR2B-containing N-methyl-D-aspartate receptors and prevents glutamate-induced cell death. J. Biol. Chem. 281, 34859–34869.
He, K., Song, L., Cummings, L.W., Goldman, J., Huganir, R.L., Lee, H.K., 2009. Stabilization of Ca2+-permeable AMPA receptors at perisynaptic sites by GluR1-S845 phosphorylation. Proc. Natl. Acad. Sci. U. S. A. 106, 20033–20038.
Henley, J.M., 2003. Proteins interactions implicated in AMPA receptor trafficking: a clear destination and an improving route map. Neurosci. Res.
Henley, J.M., Wilkinson, K.A., 2013. AMPA receptor trafficking and the mechanisms underlying synaptic plasticity and cognitive aging. Dialogues Clin. Neurosci. 15, 11–27.
Huganir, R.L., Nicoll, R.A., 2013. AMPARs and synaptic plasticity: the last 25 years. Neuron.
Ichikawa, Y., Ghanefar, M., Bayeva, M., Wu, R., Khechaduri, A., Naga Prasad, S.V., Mutharasan, R.K., Jairaj Naik, T., Ardehali, H., 2014. Cardiotoxicity of doxorubicin is mediated through mitochondrial iron accumulation. J. Clin. Invest. 124, 617–630.
Inagaki, M., Yoshikawa, E., Matsuoka, Y., Sugawara, Y., Nakano, T., Akechi, T., Wada, N., Imoto, S., Murakami, K., Uchitomi, Y., Kobayakawa, M., Akizuki, N., Fujimori, M., 2007. Smaller regional volumes of brain gray and white matter demonstrated in breat cancer survivors exposed to adjuvant chemotherapy. Cancer 109, 146–156.
Jenkins, V., Shilling, V., Deutsch, G., Bloomfield, D., Morris, R., Allan, S., Bishop, H., Hodson, N., Mitra, S., Sadler, G., Shah, E., Stein, R., Whitehead, S., Winstanley, J., 2006. A 3-year prospective study of the effects of adjuvant treatments on cognition in women with early stage breast cancer. Br. J. Cancer 94, 828–834.
Jia, Z., Agopyan, N., Miu, P., Xiong, Z., Henderson, J., Gerlai, R., Taverna, F.A., Velumian, A., MacDonald, J., Carlen, P., Abramow-Newerly, W., Roder, J., 1996. Enhanced LTP in mice deficient in the AMPA receptor GluR2. Neuron 17, 945–956.
Johnson, M.W., Chotiner, J.K., Watson, J.B., 1997. Isolation and characterization of synaptoneurosomes from single rat hippocampal slices. J. Neurosci. Methods 77, 151–156.
Keeney, J.T.R., Ren, X., Warrier, G., Noel, T., Powell, D.K., Brelsfoard, J.M., Sultana, R., Saatman, K.E., St.Clair, D.K., Butterfield, D.A., 2018. Doxorubicin-induced elevated oxidative stress and neurochemical alterations in brain and cognitive decline: protection by MESNA and insights into mechanisms of chemotherapy-induced cognitive impairment ("chemobrain"). Oncotarget 9, 30324–30339.
Kesler, S.R., Blayney, D.W., 2016. Neurotoxic effects of anthracycline- vs nonanthracycline-based chemotherapy on cognition in breast cancer survivors. JAMA Oncol. 2, 185–192.
Kitamura, Y., Hattori, S., Yoneda, S., Watanabe, S., Kanemoto, E., Sugimoto, M., Kawai, T., Machida, A., Kanzaki, H., Miyazaki, I., Asanuma, M., Sendo, T., 2015. Doxorubicin and cyclophosphamide treatment produces anxiety-like behavior and spatial cognition impairment in rats: possible involvement of hippocampal neurogenesis via brain-derived neurotrophic factor and cyclin D1 regulation. Behav. Brain Res. 292, 184–193.
Konat, G.W., Kraszpulski, M., James, I., Zhang, H.T., Abraham, J., 2008. Cognitive dysfunction induced by chronic administration of common cancer chemotherapeutics in rats. Metab. Brain Dis. 23, 325–333.
Korz, V., Frey, J.U., 2003. Stress-related modulation of hippocampal long-term potentiation in rats: involvement of adrenal steroid receptors. J. Neurosci. 23, 7281–7287.
Kraeuter, A.K., Guest, P.C., Sarnyai, Z., 2019. The Y-maze for assessment of spatial working and reference memory in mice. In: Methods in Molecular Biology. Humana Press Inc., pp. 105–111
Lahoti, S., Patel, T.D., Thekkemadom, V., Beckett, R., Ray, D.S., 2012. Doxorubicin-induced in vivo nephrotoxicity involves oxidative stress- mediated multiple pro- and anti-apoptotic signaling pathways. Curr. Neurovasc. Res. 9, 282–295.
Lakshminarasimhan, H., Coughlin, B.L., Darr, A.S., Byrne, J.H., 2017. Characterization and reversal of Doxorubicin-mediated biphasic activation of ERK and persistent excitability in sensory neurons of Aplysia californica. Sci. Rep. 7, 1–14.
Lambert, M., Ouimet, L.A., Wan, C., Stewart, A., Collins, B., Vitoroulis, I., Bielajew, C., 2018. Cancer-related cognitive impairment in breast cancer survivors: an examination of conceptual and statistical cognitive domains using principal component analysis. Oncol. Rev.
Lange, M., Joly, F., 2017. How to identify and manage cognitive dysfunction after breast cancer treatment. J. Oncol. Pract. 13, 784–790.
Lee, H.K., 2006. AMPA receptor phosphorylation in synaptic plasticity: insights from knockin mice. In: The Dynamic Synapse: Molecular Methods in Ionotropic Receptor Biology. CRC Press, pp. 261–278.
Levenga, J., Wong, H., Milstead, R.A., Keller, B.N., Laplante, L.E., Hoeffer, C.A., 2017. AKT isoforms have distinct hippocampal expression and roles in synaptic plasticity. Elife 6.
Li, X., Lu, Y., Liang, K., Liu, B., Fan, Z., 2005. Differential responses to doxorubicin-induced phosphorylation and activation of Akt in human breast cancer cells. Breast Cancer Res. 7, R589.
Lüscher, C., Malenka, R.C., 2012. NMDA receptor-dependent long-term potentiation and long-term depression (LTP/LTD). Cold Spring Harb. Perspect. Biol. 4.
Lynch, G., 2002. Memory enhancement: the search for mechanism-based drugs. Nat. Neurosci.

Lynch, G., Gall, C.M., 2006. Ampakines and the threefold path to cognitive enhancement. Trends Neurosci. 29, 554–562.
Malenka, R.C., Nicoll, R.A., 1993. NMDA-receptor-dependent synaptic plasticity: multiple forms and mechanisms. Trends Neurosci.
Malinow, R., 2003. AMPA receptor trafficking and long-term potentiation. Philos. Trans. R. Soc. B Biol. Sci.
Malinow, R., Malenka, R.C., 2002. AMPA receptor trafficking and synaptic plasticity. Annu. Rev. Neurosci.
McCubrey, J.A., Steelman, L.S., Chappell, W.H., Abrams, S.L., Wong, E.W.T., Chang, F., Lehmann, B., Terrian, D.M., Milella, M., Tafuri, A., Stivala, F., Libra, M., Basecke, J., Evangelisti, C., Martelli, A.M., Franklin, R.A., 2007. Roles of the Raf/MEK/ERK pathway in cell growth, malignant transformation and drug resistance. Biochim. Biophys. Acta Mol. Cell Res.
Meng, F., Guo, J., Zhang, Q., Song, B., Zhang, G., 2003. Autophosphorylated calcium/calmodulin-dependent protein kinase II alpha (CaMKII alpha) reversibly targets to and phosphorylates N-methyl-D-aspartate receptor subunit 2B (NR2B) in cerebral ischemia and reperfusion in hippocampus of rats. Brain Res. 967, 161–169.
Nakata, H., Nakamura, S., 2007. Brain-derived neurotrophic factor regulates AMPA receptor trafficking to post-synaptic densities via IP3R and TRPC calcium signaling. FEBS Lett. 581, 2047–2054.
Nogueira, V., Park, Y., Chen, C.C., Xu, P.Z., Chen, M.L., Tonic, I., Unterman, T., Hay, N., 2008. Akt determines replicative senescence and oxidative or oncogenic premature senescence and sensitizes cells to oxidative apoptosis. Cancer Cell 14, 458–470.
Ogden, K.K., Chen, W., Swanger, S.A., McDaniel, M.J., Fan, L.Z., Hu, C., Tankovic, A., Kusumoto, H., Kosobucki, G.J., Schulien, A.J., Su, Z., Pecha, J., Bhattacharya, S., Petrovski, S., Cohen, A.E., Aizenman, E., Traynelis, S.F., Yuan, H., 2017. Molecular mechanism of disease-associated mutations in the pre-M1 helix of NMDA receptors and potential rescue pharmacology. PLoS Genet. 13, e1006536.
Oh, M.C., Derkach, V.A., Guire, E.S., Soderling, T.R., 2006. Extrasynaptic membrane trafficking regulated by GluR1 serine 845 phosphorylation primes AMPA receptors for long-term potentiation. J. Biol. Chem. 281, 752–758.
Ozawa, S., 2009. Ca2+-permeable AMPA receptors in central neurons. J. Physiol. 587, 1861–1862.
Parameshwaran, K., Sims, C., Kanju, P., Vaithianathan, T., Shonesy, B.C., Dhanasekaran, M., Bahr, B.A., Suppiramaniam, V., 2007. Amyloid beta-peptide Abeta(1-42) but not Abeta(1-40) attenuates synaptic AMPA receptor function. Synapse 61, 367–374.
Parameshwaran, K., Buabeid, M.A., Karuppagounder, S.S., Uthayathas, S., Thiruchelvam, K., Shonesy, B., Dityatev, A., Escobar, M.C., Dhanasekaran, M., Suppiramaniam, V., 2012. Developmental nicotine exposure induced alterations in behavior and glutamate receptor function in hippocampus. Cell. Mol. Life Sci. 69, 829–841.
Parameshwaran, K., Buabeid, M.A., Bhattacharya, S., Uthayathas, S., Kariharan, T., Dhanasekaran, M., Suppiramaniam, V., 2013. Long term alterations in synaptic physiology, expression of β2 nicotinic receptors and ERK1/2 signaling in the hippocampus of rats with prenatal nicotine exposure. Neurobiol. Learn. Mem. 106, 102–111.
Petrisko, T.J., Bloemer, J., Pinky, P.D., Srinivas, S., Heslin, R.T., Du, Y., Setti, S.E., Hong, H., Suppiramaniam, V., Konat, G.W., Reed, M.N., 2020. Neuronal CXCL10/CXCR3 Axis mediates the induction of cerebral hyperexcitability by peripheral viral challenge. Front. Neurosci. 14.
Radin, D.P., Purcell, R., Lippa, A.,S., 2018a. Oncolytic properties of ampakines in vitro. Anticancer Res. 38.
Radin, D.P., Rogers, G.A., Hewitt, K.E., Purcell, R., Lippa, A., 2018b. Ampakines attenuate staurosporine-induced cell death in primary cortical neurons: implications in the 'chemo-brain' phenomenon. Anticancer Res. 38, 3461–3466.
Riedel, G., Platt, B., Micheau, J., 2003. Glutamate receptor function in learning and memory. Behav. Brain Res.
Salas-Ramirez, K.Y., Bagnall, C., Frias, L., Abdali, S.A., Ahles, T.A., Hubbard, K., 2015. Doxorubicin and cyclophosphamide induce cognitive dysfunction and activate the ERK and AKT signaling pathways. Behav. Brain Res. 292, 133–141.
Sarnyai, Z., Sibille, E.L., Pavlides, C., Fenster, R.J., McEwen, B.S., Tóth, M., 2000. Impaired hippocampal-dependent learning and functional abnormalities in the hippocampus in mice lacking serotonin1A receptors. Proc. Natl. Acad. Sci. U. S. A. 97, 14731–14736.
Suppiramaniam, V., Vaithianathan, T., Parameshwaran, K., 2006. Electrophysiological analysis of interactions between carbohydrates and transmitter receptors reconstituted in lipid bilayers. Methods Enzymol. 417, 80–90.
Thomas, T.C., Beitchman, J.A., Pomerleau, F., Noel, T., Jungsuwadee, P., Allan Butterfield, D., Clair, D.K.S., Vore, M., Gerhardt, G.A., 2017. Acute treatment with doxorubicin affects glutamate neurotransmission in the mouse frontal cortex and hippocampus. Brain Res. 1672, 10–17.
Thorn, C.F., Oshiro, C., Marsh, S., Hernandez-Boussard, T., McLeod, H., Klein, T.E., Altman, R.B., 2011. Doxorubicin pathways: pharmacodynamics and adverse effects. Pharmacogenetics Genom. 21, 440–446.
Tomita, S., Adesnik, H., Sekiguchi, M., Zhang, W., Wada, K., Howe, J.R., Nicoll, R.A., Bredt, D.S., 2005. Stargazin modulates AMPA receptor gating and trafficking by distinct domains. Nature 435, 1052–1058.
Traynelis, S.F., Wollmuth, L.P., McBain, C.J., Menniti, F.S., Vance, K.M., Ogden, K.K., Hansen, K.B., Yuan, H., Myers, S.J., Dingledine, R., 2010. Glutamate receptor ion channels: structure, regulation, and function. Pharmacol. Rev.
Understanding Post-Treatment, 2017. "Chemobrain" - National Cancer Institute [WWW Document]. https://www.cancer.gov/about-cancer/treatment/research/understanding-chemobrain. (Accessed 15 April 2020).
Vaithianathan, T., Manivannan, K., Kleene, R., Bahr, B.A., Dey, M.P., Dityatev, A., Suppiramaniam, V., 2005. Single channel recordings from synaptosomal AMPA receptors. Cell Biochem. Biophys. 42, 75–85.
Wu, J., Guo, W., Lin, S.Z., Wang, Z.J., Kan, J.T., Chen, S.Y., Zhu, Y.Z., 2016. Gp130-mediated STAT3 activation by s-propargyl-cysteine, an endogenous hydrogen sulfide initiator, prevents doxorubicin-induced cardiotoxicity. Cell Death Dis. 7, e2339.
Zhang, S., Liu, X., Bawa-Khalfe, T., Lu, L.S., Lyu, Y.L., Liu, L.F., Yeh, E.T.H., 2012. Identification of the molecular basis of doxorubicin-induced cardiotoxicity. Nat. Med. 18, 1639–1642.
Zhang, H., Zhang, C., Vincent, J., Zala, D., Benstaali, C., Sainlos, M., Grillo-Bosch, D., Daburon, S., Coussen, F., Cho, Y., David, D.J., Saudou, F., Humeau, Y., Choquet, D., 2018. Modulation of AMPA receptor surface diffusion restores hippocampal plasticity and memory in Huntington's disease models. Nat. Commun. 9.